Application of steering filters to localized anisotropic tomography with well data

Andrey Bakulin, Marta Woodward, Yangjun (Kevin) Liu, Olga Zdraveva, Dave Nichols, Konstantin Osypov*
WesternGeco

Summary

Estimation of anisotropic parameters for depth models requires some type of joint inversion of seismic and borehole data. We demonstrate that conventional grid reflection tomography can be adapted to simultaneously invert for all parameters of a local 3D anisotropic model. Success requires three key ingredients: jointly invert seismic and well data, localize tomography to a small volume around the borehole, and steer the updates along seismic horizons with steering filters. We describe steering filters and demonstrate 3D anisotropic tomography regularized with steering-filter preconditioners on a synthetic data set.

Introduction

Depth imaging with vertically transversely isotropic (VTI) models requires estimation of three model parameters. Whereas the vertical velocity V_{P0} is usually obtained using seismic reflection tomography, the Thomsen parameters δ and ε are more often estimated by other methods (Bear et al., 2005; Bakulin et al., 2010). Manual inversion using a combination of seismic and well data is popular for 1D models, but no commonly accepted industry approach exists for 3D models and deviated wells. We demonstrate that localized seismic tomography with well data can simultaneously invert for V_{P0}, ε, and δ, when it is regularized with steering-filter preconditioners.

Steering filters

Surface seismic data may be used to produce accurate isotropic earth velocity models when the data are dense and the earth is well-illuminated by rays at a wide range of angles. When the earth is anisotropic, well measurements must be added to further constrain the problem. Other a priori geological information may also be needed to shape the earth model. The shaping may be imposed before a tomographic velocity analysis – as with decomposition of the problem into interpreted layers and volumes, or by defining fixed Thomsen parameter fields from independent well analyses, - or the shaping may be imposed during the tomography with the method of preconditioning (Harlan, 1995; Fomel, 1997).

Equation 1 shows tomography formulated with preconditioning

$$\mathbf{LS}\Delta\boldsymbol{\alpha}' = \Delta\mathbf{d} \qquad (1)$$

(Woodward et al., 1998, 2008). $\Delta\mathbf{d}$ is the data misfit vector, corresponding to residual moveout, well misties, etc. The $\mathbf{L}$ matrix operator contains the $\partial\mathbf{d}/\partial\alpha_i$ Frechet derivative terms describing data misfit changes as a function of property α perturbations at nodes i. The solution or property update vector is $\Delta\boldsymbol{\alpha} = \mathbf{S}\Delta\boldsymbol{\alpha}'$, where $\mathbf{S}$ is the preconditioner that constrains the shape of the update and $\Delta\boldsymbol{\alpha}'$ is the raw, uncorrelated, update vector, before shaping by the preconditioner. $\mathbf{S}$ is a factored form of an a priori assumed covariance matrix (Harlan, 1995).

When the data measurements constrain the tomography problem well, it is reasonable to implement the preconditioner as a 3D isotropic smoother. We generally use a 3D smoother that varies in X and Y as a function of depth to produce the smoothest possible model that will flatten our gathers (Woodward et al, 2008). When the data are insufficient to constrain the tomography problem, we use the steering filters described by Clapp et al. (1998). We create the filters in three steps. First, we produce a 3D dip field that we want our update to follow, either by picking dip from a seismic stack or by interpolating dip between horizons created by an imaginative interpreter. Second, we build a set of dip annihilator filters covering the dip range in the targeted dip field. Finally, we invert these filters to create dip steering filters using the helix transform (Claerbout, 1998). When we apply a preconditioner $\mathbf{S}$ composed of steering filters to our property update vector, we directionally smooth our update at each location along the dip corresponding to that location in our a priori dip field.

We illustrate the use of steering filters to constrain an underdetermined tomography problem that simultaneously inverts for all three parameters of a VTI model around and away from a well.

Synthetic example

Let us perform localized anisotropic tomography with steering filters to invert for the 2.5D synthetic model shown in Figure 1. The model has 49 reflectors that have constant

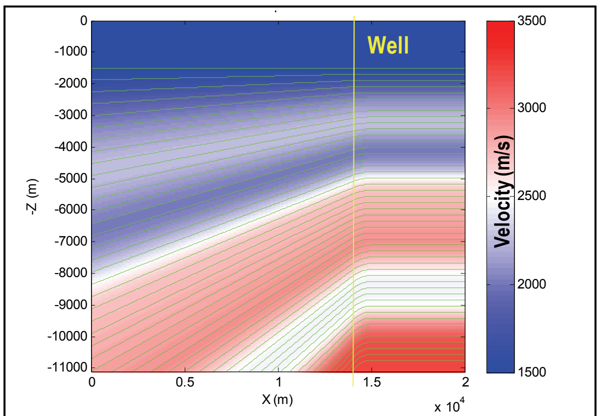

Figure 1: Vertical velocity (V_{P0}) of the VTI velocity model with 49 reflecting horizons used for synthetic generation. Note conformance of velocity to reflector geometry.

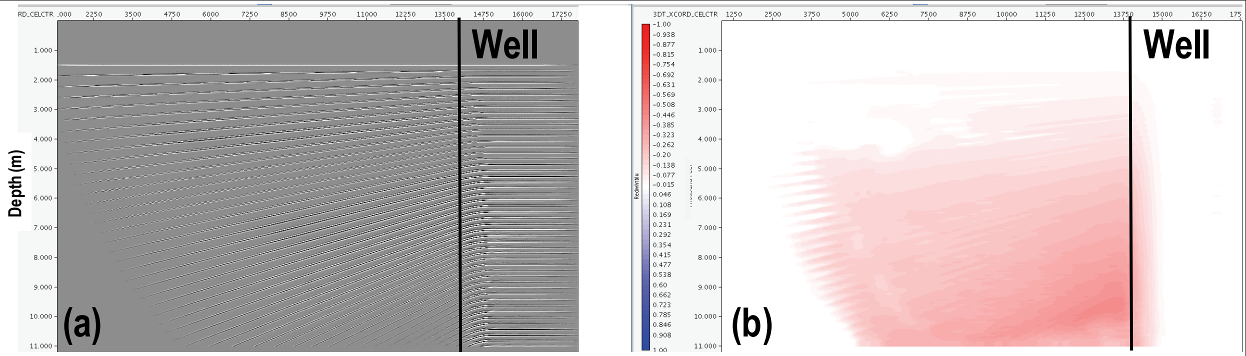

Figure 2: Stacked image (a) and corresponding smoothed dip field (b) obtained with the initial model. Inline dip filed is shown as a tangent of the geological dip angle. This dip field was used for steering paramater updates in all iterations of tomography.

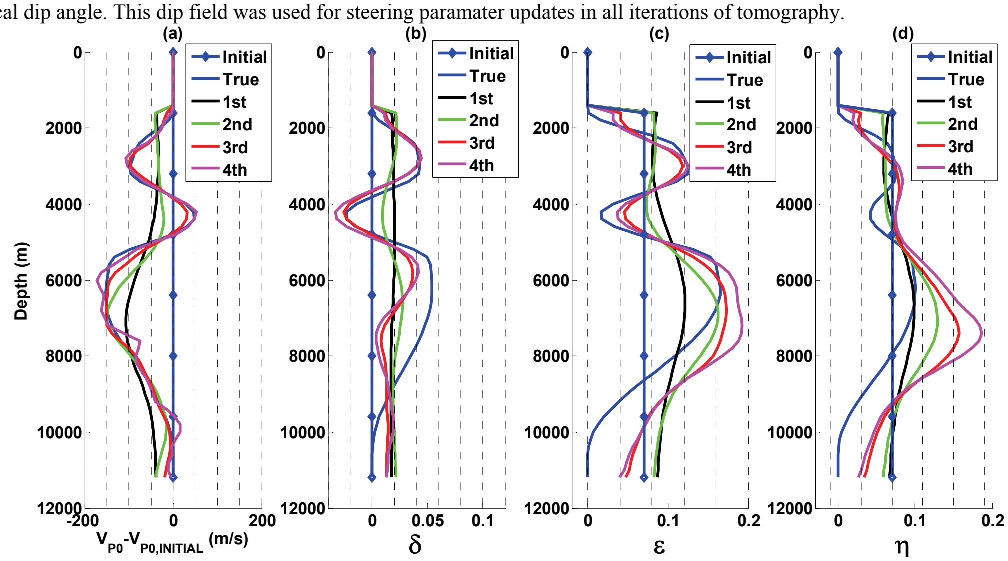

Figure 3: Results of a three-parameter VTI tomography (V_{P0}, ε, and δ) using seismic and vertical checkshot data. Velocity and anisotropy profiles after each iteration are shown together with the initial and true models: (a) update in velocity shown as a difference between current velocity at each iteration and initial velocity profile; (b) δ; (c) ε; (d) η.

dip to the left of the well located at X=14 km. The reflector dip increases from 0° at the water bottom to 35° at depth.
The V_{P0}, ε, and δ fields vary smoothly vertically (Figure 3) and conform laterally in dip with the seismic reflectors (Figures 1, 6a, 6b, 6c). The reflectors correspond to density contrasts and the seismic data are computed with anisotropic ray tracing. To succeed with a multiparameter inversion for V_{P0}, ε, and δ, we have to introduce three key ingredients. First, we have to jointly invert seismic and well data as described by Bakulin et al (2009), because, without the well data, the inversion is completely nonunique. In this example, we use a checkshot survey that consists of 191 measurement depths, one every 50 m starting at the water bottom. Second, we localize tomography to the area around the well where we may assume that the borehole data remains applicable. In our example, we achieve this by using only 51 common-image-point (CIP) gathers in a ±1,000 m aperture around the well. Third, we constrain the parameter updates to follow the local geological layering by applying preconditioning with steering filters. This approach propagates the well information (velocity) away from the well; whereas, at the same time, it makes determination of the anisotropic parameters unique. While the checkshot traveltimes constrain vertical velocity at the well, the moveout of the surface seismic data requires the local dip information to uniquely and stably determine δ and ε.

The initial model has constant Thomsen parameter fields (δ=0 and ε=0.07) and a variable V_{P0} equal to stacking velocity computed with a 1D approximation corresponding to isotropic velocity analysis. Figure 2 shows the somewhat unfocused starting image produced with this model. The dip field used for construction of the steering-filter preconditioners is shown in Figure 2b. For this synthetic study, we used the same dip field for all iterations of the tomography, although it may have been better to repick it each time.

Figure 3 shows the anisotropic parameter profiles along the vertical well as recovered by four iterations of tomography. Figure 4a shows, that the initial V_{P0} is too fast as manifested by checkshot residuals of up to 85 ms. The first two iterations recover the smooth trends of the velocity and anisotropy fields; resolution is refined in the final two iterations (Figure 3). While tomography makes global adjustments to velocity to match the checkshot traveltimes (Figure 4b), it also keeps increasing the Thomsen parameters to flatten the CIP gathers (Figure 3bc). Overall, the tomography recovers a good estimate of the anisotropic parameters around the well. Below 6,000 m we observe some inaccuracies in the Thomsen parameters (Figure 3bc) that may be due to ambiguity between δ and ε caused by reduction of the reflection half-opening angle from 50º at 6,000 m to 25º at 12,000 m. Errors were also introduced by our failure to update the dip field used for the steering-filter and ray-tracing calculations at each iteration.

The fundamental importance of the steering filters for tomography convergence can be seen in Figure 5, where we compare first iteration tomographic updates produced with and without steering filters. Multiparameter inversion for V_{P0}, ε, and δ is highly non-unique without the constraint of geological dip. Despite performing preconditioning using a 5-km horizontal smoother in the test without steering filters, we immediately observe large localized hot spots in the parameter updates (Figure 5a). While velocity at the well will eventually be resolved correctly due to the checkshot constraint, this will be achieved by having a bull's eye (Figure 5a). Likewise, anisotropy away from the well will look like a checkerboard. Anisotropic parameters along the well will also be incorrect because, in contrast to vertical velocity constrained by zero-offset checkshot traveltimes, Thomsen's δ and ε are determined from a combination of small, medium, and large offsets. We observe quite different behavior for the dip-guided updates: the first-iteration steering-filter results of Figures 5d, 5e, 5f are already converging to the correct solution. After performing four iterations of tomography and gradually increasing the resolution of the steering-filter preconditioner, we recover the model property fields shown in Figure 6. While not perfect, they provide a reasonable result that is acceptable for practical anisotropic model building. They demonstrate that recovery of even a 2D anisotropic model requires more than just vertical checkshot and surface-seismic data, and that an assumption of property conformance to reflector dip is one solution to the problem.

Discussion

Preconditioning with steering filters is not a computational trick that turns a non-unique inverse problem into a unique one. Rather it is a tool to convey to the solver our geological belief that anisotropy is controlled by lithology (Bear et al., 2005; Bakulin et al., 2010). If this is indeed the case, then borehole-constrained tomography with steering-filter preconditioning allows us to conveniently obtain estimates of anisotropy in structurally complex environments. Data from deviated boreholes (sonic logs, checkshot, VSP, markers, and others) can be included with ease, and extension to tilted transverse isotropy (TTI) is trivial. The method may also be used to invert multiple wells with regional surface seismic data simultaneously, extrapolating properties between wells along the interpreted dip. However, if anisotropy is controlled by something other than lithology, then steering-filter preconditioning along the dip may produce a false solution. A different constraint may be required.

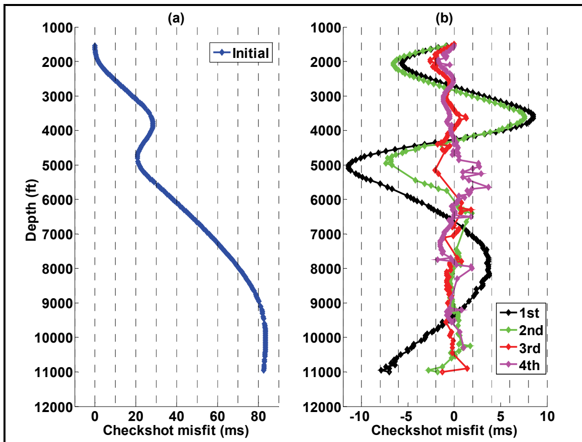

Figure 4: Misfit in checkshot traveltimes for initial model (a) and all subsequent tomography iterations (b). Misfit is computed as a difference between measured and predicted traveltimes.

Conclusions

We have presented a case study of localized anisotropic tomography that jointly inverts for V_{P0}, ε, and δ around a vertical well placed on the flank of an anticlinal structure. Preconditioning with steering filters in the tomography shapes the updates so that they conform to the geological dip. This geologically consistent regularization allows us to derive reasonably good estimates of the anisotropic parameters in a 2.5D synthetic model. There are multiple practical advantages for using conventional reflection tomography with steering filters for joint multiparameter inversion. The most important one is that all the constraints can be introduced in a flexible way using the same gridded model without a need to build or regrid the model every time, as is the requirement in many other techniques with structurally imposed constraints.

Localized anisotropic tomography with steering filters allows the 3D calibration of VTI and TTI anisotropic models in structurally complex areas, while at the same time enabling incorporation of well data from deviated boreholes. Anisotropic profiles derived by local tomography at single wells can be propagated between wells using horizon-guided interpolation (Bakulin et al., 2010). Alternatively, global tomography using data from multiple wells with dip-guided steering-filter preconditioning may more automatically recover 3D anisotropic parameter fields between wells. Multiparameter inversion may still have some nonuniqueness. Once joint tomography brings us close to the correct model, the nonuniqueness may be explored and eliminated by minor manual interactive updates or by a supplemental run of tomography with uncertainty analysis (Bakulin et al, 2009b).

Acknowledgements

We thank Dmitry Alexandrov (summer intern from St. Petersburg State University) for help with generating the synthetic dataset.

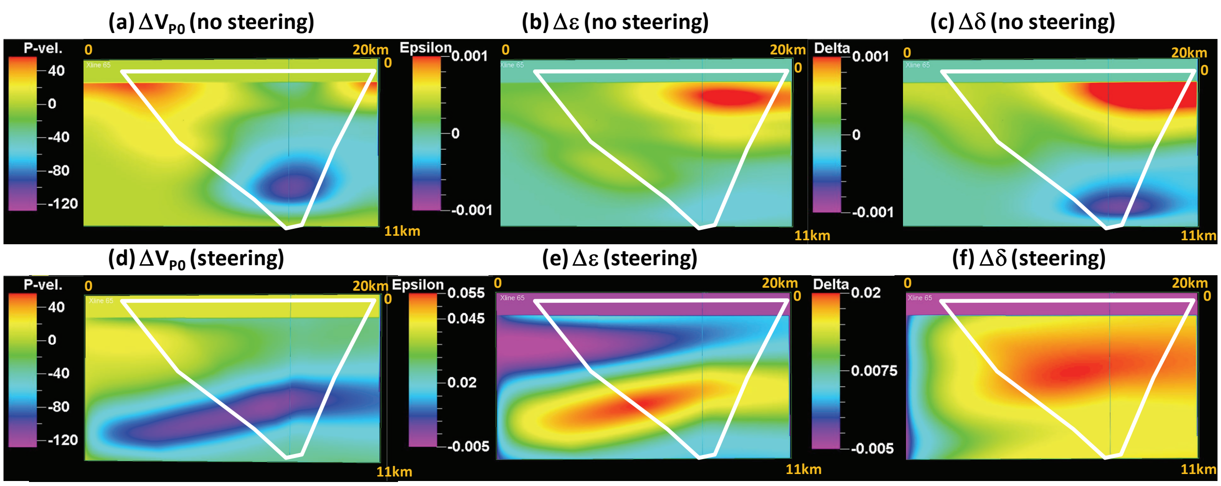

Figure 5: Velocty and anisotropy updates without (a-c) and with steerfing filter (d-f) obtained by joint tomography of seismic and checkshot data. White outline shows the area of significant hitcount that is limited by use of 51 CIP gathers in the area ±1000 m around the well. Observe laterally incoherent hot spots in unsteered update (a-c). In contrast, steering filter only allows the updates that are conformable to subsurface layers (d-f) seen in Figure 1 and 2.

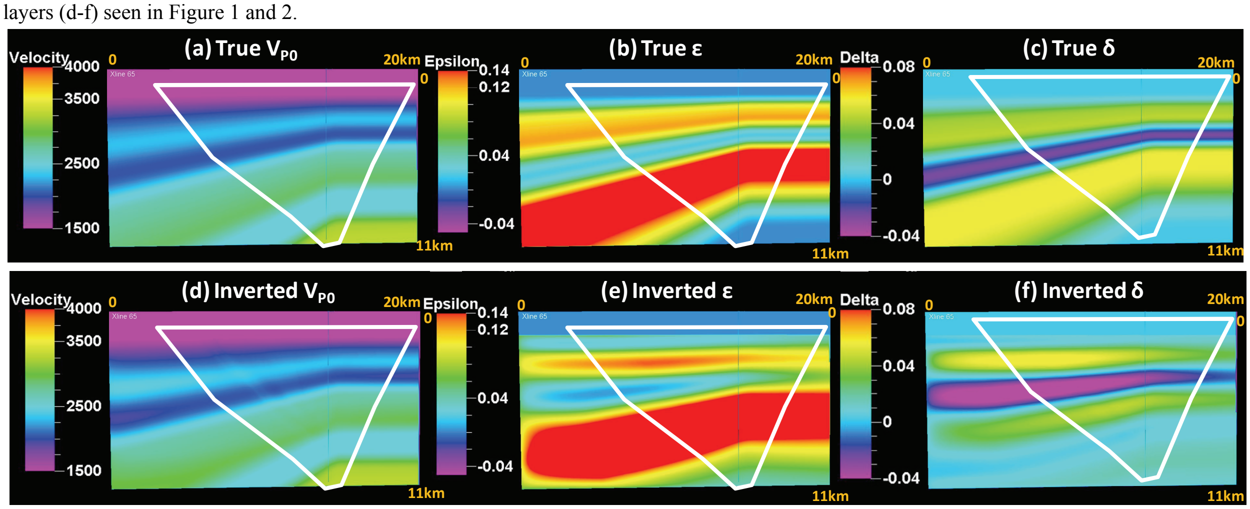

Figure 6: True velocity model (a-c) versus inverted velocity model (d-f) obtained by joint tomography of seismic and checkshot data with the steering filter. White outline shows the area of significant hitcount that is limited by use of 51 CIP gathers in the area ±1000 m around the well. Observe conformance of recovered properties to geological layers seen in Figure 1 and 2.

EDITED REFERENCES

Note: This reference list is a copy-edited version of the reference list submitted by the author. Reference lists for the 2010 SEG Technical Program Expanded Abstracts have been copy edited so that references provided with the online metadata for each paper will achieve a high degree of linking to cited sources that appear on the Web.

REFERENCES

Bakulin, A., Y. Liu, and O. Zdraveva, 2010, Borehole-calibrated and Geologically Plausible Anisotropic Models Using Wells and Horizon-guided Interpolation: 72nd EAGE Conference and Exhibition, Extended Abstracts, C038.

Bakulin, A., M. Woodward, D. Nichols, K. Osypov, and O. Zdraveva, 2009a, Localized anisotropic tomography with well information in VTI media: 79th Annual International Meeting, SEG, Expanded Abstracts, 221-225.

Bakulin, A., M. Woodward, D. Nichols, K. Osypov, and O. Zdraveva, 2009b, Anisotropic model building with uncertainty analysis: 79th Annual International Meeting, SEG, Expanded Abstracts, 3720-3724.

Bear, L. K., T. A. Dickens, J. R. Krebs, J. Liu, and P. Traynin, 2005, Integrated velocity model estimation for improved positioning with anisotropic PSDM: The Leading Edge, **24**, no. 6, 622–634, doi:10.1190/1.1946219.

Claerbout, J., 1998, Multidimensional recursive filters via a helix: 68th Annual International Meeting, SEG, Expanded Abstracts, 1532-1541.

Clapp, R., and B. Biondi, B., Fomel, S., and J. Claerbout, 1998, Regularizing velocity estimation using geologic dip information: 68th Annual International Meeting, SEG, Expanded Abstracts, 1850-1853.

Fomel, S., 1997, On model-space and data-space regularization: A tutorial: Stanford Exploration Project Report, **94**, 141–160.

Harlan, W. S., 1995, Regularization by model reparameterization: http://billharlan.com/pub/papers/regularization.html, accessed March 31, 2010.

Woodward, M., D. Nichols, O. Zdraveva, P. Whitfield, and T. Johns, 2008, A decade of tomography: Geophysics, **73**, no. 5, VE5–VE11, doi:10.1190/1.2969907.

Woodward, M., and P. Farmer, P., D. Nichols, and S. Charles, 1998, Automated 3D tomographic velocity analysis of residual moveout in prestack depth migrated common image point gathers: 68th Annual International Meeting, SEG, Expanded Abstracts, 1218–1221.